

Bowdoin College

## Bowdoin Digital Commons

---

Chemistry Faculty Publications

Faculty Scholarship and Creative Work

---

11-7-2017

### MnNiO<sub>3</sub> revisited with modern theoretical and experimental methods

Allison L. Dzubak

*Oak Ridge National Laboratory*

Chandrima Mitra

*Oak Ridge National Laboratory*

Michael Chance

*Oak Ridge National Laboratory*

Stephen Kuhn

*Oak Ridge National Laboratory*

Gerald E. Jellison

*Oak Ridge National Laboratory*

*See next page for additional authors*

Follow this and additional works at: <https://digitalcommons.bowdoin.edu/chemistry-faculty-publications>

---

#### Recommended Citation

Dzubak, Allison L.; Mitra, Chandrima; Chance, Michael; Kuhn, Stephen; Jellison, Gerald E.; Sefat, Athena S.; Krogel, Jaron T.; and Reboledo, Fernando A., "MnNiO<sub>3</sub> revisited with modern theoretical and experimental methods" (2017). *Chemistry Faculty Publications*. 17.

<https://digitalcommons.bowdoin.edu/chemistry-faculty-publications/17>

This Article is brought to you for free and open access by the Faculty Scholarship and Creative Work at Bowdoin Digital Commons. It has been accepted for inclusion in Chemistry Faculty Publications by an authorized administrator of Bowdoin Digital Commons. For more information, please contact [mdoyle@bowdoin.edu](mailto:mdoyle@bowdoin.edu), [a.sauer@bowdoin.edu](mailto:a.sauer@bowdoin.edu).

---

**Authors**

Allison L. Dzubak, Chandrima Mitra, Michael Chance, Stephen Kuhn, Gerald E. Jellison, Athena S. Sefat, Jaron T. Krogel, and Fernando A. Reboredo

RESEARCH ARTICLE | NOVEMBER 03 2017

## MnNiO<sub>3</sub> revisited with modern theoretical and experimental methods

Allison L. Dzubak; Chandrima Mitra; Michael Chance; ... et. al



*J. Chem. Phys.* 147, 174703 (2017)

<https://doi.org/10.1063/1.5000847>

 CHORUS



View  
Online



Export  
Citation

CrossMark

### Articles You May Be Interested In

Structure and Ferrimagnetism of the Ilmenite Compound MnNiO<sub>3</sub>

*Journal of Applied Physics* (June 2004)



Time to get excited.  
Lock-in Amplifiers – from DC to 8.5 GHz

[Find out more](#)

 Zurich  
Instruments

# MnNiO<sub>3</sub> revisited with modern theoretical and experimental methods

Allison L. Dzubak, Chandrima Mitra, Michael Chance, Stephen Kuhn, Gerald E. Jellison, Jr., Athena S. Sefat, Jaron T. Krogel, and Fernando A. Reboredo<sup>a)</sup>

*Materials Science and Technology Division, Oak Ridge National Laboratory, Oak Ridge, Tennessee 37831, USA*

(Received 18 August 2017; accepted 20 October 2017; published online 3 November 2017)

MnNiO<sub>3</sub> is a strongly correlated transition metal oxide that has recently been investigated theoretically for its potential application as an oxygen-evolution photocatalyst. However, there is no experimental report on critical quantities such as the band gap or bulk modulus. Recent theoretical predictions with standard functionals such as LDA+U and HSE show large discrepancies in the band gaps (about 1.23 eV), depending on the nature of the functional used. Hence there is clearly a need for an accurate quantitative prediction of the band gap to gauge its utility as a photocatalyst. In this work, we present a diffusion quantum Monte Carlo study of the bulk properties of MnNiO<sub>3</sub> and revisit the synthesis and experimental properties of the compound. We predict quasiparticle band gaps of 2.0(5) eV and 3.8(6) eV for the majority and minority spin channels, respectively, and an equilibrium volume of 92.8 Å<sup>3</sup>, which compares well to the experimental value of 94.4 Å<sup>3</sup>. A bulk modulus of 217 GPa is predicted for MnNiO<sub>3</sub>. We rationalize the difficulty for the formation of ordered ilmenite-type structure with specific sites for Ni and Mn to be potentially due to the formation of antisite defects that form during synthesis, which ultimately affects the physical properties of MnNiO<sub>3</sub>. *Published by AIP Publishing.* <https://doi.org/10.1063/1.5000847>

## I. INTRODUCTION

Transition metal oxides (TMOs) show a wide range of useful and tunable physical properties that include magnetism, superconductivity, or ferroelectricity. As such, they form the building blocks and find applications in most technologically important devices. Therefore, a fundamental understanding of TMO properties is crucial, and this is where computational modeling plays an important role. MnNiO<sub>3</sub> is one such TMO material that has recently been theoretically investigated for its potential application as an oxygen-evolution photocatalyst.<sup>1</sup> A very interesting feature of MnNiO<sub>3</sub> is that it has two transition metal ions, Mn and Ni, both of which have partially filled *d* orbitals. Therefore, MnNiO<sub>3</sub> is at the crossroads of two very important families of highly correlated materials that have received intense attention: the nickelates and manganites.

An accurate theoretical study of this material requires an approach beyond that of the standard band approaches. The broadly applied density functional theory (DFT) could in principle be exact; however, common approximations of the density functional, e.g., the local density approximation (LDA)<sup>2</sup> and semi-local generalized gradient approximation (GGA)<sup>3</sup> do not account for all experimental observations without adjustable parameters. In general, those approximations fail to describe the electronic gap of strongly correlated systems (see Ref. 4 and reference therein) because of the so-called self-interaction or delocalization error. The DFT+U method is commonly used to correct for these errors with a

Hubbard-type model.<sup>5–7</sup> The theoretical calculations of MnNiO<sub>3</sub> show large variations in the computed band gaps depending on the nature of the functional used for the calculation. For example, the computed band gap using the Perdew-Burke-Ernzerhof PBE+U functional (where U is 3.9 eV and 6.2 eV for Mn and Ni, respectively) was found to be 1.75 eV, while the Heyd-Scuseria-Ernzerhof (HSE) functional yielded a gap of 2.98 eV.<sup>1</sup> Furthermore, the use of functionals such as the HSE requires an adequate choice of the mixing parameter  $\alpha$  which needs to be determined empirically if accurate values are to be obtained. The same applies for the PBE+U functional, where the choice of the U parameter could be somewhat arbitrary.<sup>8</sup> Hence this reliance on empiricism poses limitations on the quantitative prediction of the band gap of any material whose experimental value is unknown. While usual DFT approximations encounter problems in TMOs, quantum Monte Carlo (QMC) solutions of the full many-electron problem—without adjustable parameters—have recently become practical for bulk TMOs and have provided accurate values for defect formation energies in multiple oxides.<sup>9–13</sup> We discuss in more detail the accuracy of DFT compared with QMC in Secs. III and IV.

Previous experimental reports suggest that although MnNiO<sub>3</sub> crystallizes in the ilmenite-type structure (space group *R*-3), oxygen vacancies are known to exist.<sup>14</sup> The activation energy of MnNiO<sub>2.98</sub> was estimated using conductivity and thermopower results as 1.4 eV.<sup>14</sup> In rhombohedral MnNiO<sub>3</sub>, both the Mn and Ni have an octahedral environment, and Mn and Ni are expected to be in +4 and +2 oxidation states, respectively.<sup>15–17</sup> The ground state magnetic structure is ferrimagnetic, where the Mn and Ni sublattices are antiferromagnetically aligned with respect to each other. Mn and

<sup>a)</sup>Electronic mail: reboredo@ornl.gov

Ni have different resulting moments, which result in a net magnetic moment in the material.

In this report, we calculate some relevant properties of MnNiO<sub>3</sub> with an *ab initio* many-body method: diffusion Monte Carlo (DMC).<sup>18,19</sup> We also revisit the synthesis of MnNiO<sub>3</sub>, in order to assess its potential use as a photocatalyst. We report the details of its crystal structure and bulk magnetic susceptibility. We use DMC to investigate the equilibrium volume, bulk modulus, the quasiparticle band gap, and the formation energy of the antisite pair defect theoretically. Experimentally, although stoichiometric composition is suggested by the refinement of X-ray diffraction patterns, the ordering of the Mn and Ni cations along the crystallographic *c*-direction may not be perfect, presenting antisite defects. The gray fine-powder produced is presumably a bad metal. The Tyndall effect and off-stoichiometry presumably hinder the determination of the band gap with reflectivity measurements. We find good agreement between the DMC-computed value for the equilibrium volume and the experimental value. The rest of this paper is organized as follows: in Sec. II, we describe the experimental and theoretical methods used in this study. Results are presented in Sec. III, and we summarize our conclusions in Sec. IV.

## II. METHODOLOGY

### A. Synthesis, structure, and magnetic susceptibility

MnNiO<sub>3</sub> was synthesized following similar routes to Ref. 14. The purity of the material was checked by collecting X-ray powder diffraction on an X'Pert PRO MPD diffractometer (Cu K<sub>α1</sub> radiation); the lattice parameters, atomic sites, and their occupancies were determined by least-squares fitting within the program package WinCSD. The chemical and particle homogeneity of the powder was checked using a Hitachi S3400 scanning electron microscope operating at 20 kV and by the use of energy-dispersive X-ray spectroscopy (EDS). The temperature- and field-dependence of the magnetization were performed with a Quantum Design magnetometer using the normal and oven settings, under an applied field of 100 G; the data were collected on the powders in zero-field-cooled (zfc) and field-cooled (fc) modes.

### B. Overview of the DMC approach

In this section, we provide a brief description of the basic steps followed in a DMC calculation. A detailed description of the methodology can be found elsewhere.<sup>20,21</sup> To achieve accurate DMC ground state energies, variational Monte Carlo (VMC)<sup>22</sup> is first performed to optimize a many-body trial wave function,  $\psi_T(R)$  as

$$\psi_T(R) = e^{-[J_1(R)+J_2(R)+J_3(R)]} D^\uparrow D^\downarrow, \quad (1)$$

where  $e^{-J_1(R)}$  and  $e^{-J_2(R)}$  are the one-body and two-body Jastrow<sup>23</sup> terms, respectively. These represent the electron-ion and electron-electron correlation terms. To further improve the description of the correlation between electrons, a three-body Jastrow term is also used,  $e^{-J_3(R)}$ , which represents the electron-electron-ion correlation. The determinants  $D^\uparrow$  and  $D^\downarrow$  are for the up and down spin states, respectively. In this work, we obtain determinants  $D^\uparrow$  and  $D^\downarrow$  using orbitals from

LDA+U calculations performed with Quantum ESPRESSO.<sup>24</sup> The important step here is to optimize the Jastrow factors by minimizing the variance of the VMC energy. We next find the value of  $U$  which minimizes the DMC energy.

The resulting optimized trial wave function serves as the starting point for the subsequent production of DMC calculations. The need for DMC arises from the fact that VMC is limited by the functional form of the trial wave function,  $\psi_T(R)$ , and the ability to optimize this trial wave function. This is where DMC proves to be vital. Within DMC, the wave function is evolved according to the Schrödinger equation which is transformed into a diffusion equation in imaginary time. When the wave function evolves in imaginary time, the ground state is projected out as the higher-energy excited states decay exponentially in time. The space of electronic configurations is explored with an ensemble of configurations, which follow quasi-independent random walks. In DMC, the random walk is guided by an importance sampling approach<sup>18,25,26</sup> which makes the process more efficient. After the configurations are equilibrated, the average of their energies is statistically analyzed.

The fixed-node approximation is used to allow DMC to be applied to fermions, where the well-known sign problem is controlled by using fixed nodes from a many-body trial wave function. The nodal surface of these wave functions is determined by the zeros of the Slater determinants  $D^\uparrow$  and  $D^\downarrow$  ( $D^\uparrow D^\downarrow = 0$ ) as indicated in Eq. (1). This approximation is variational where nodal errors only increase the DMC energy. Another approximation arises from the use of pseudopotentials. All-electron calculations are computationally very demanding and often impractical for QMC calculations. In Sec. II C, we describe the pseudopotentials used in our calculations and the various tests that are performed for validation.

The accuracy of DMC is also affected by errors introduced by a finite simulation cell. The simulation cell is subject to periodic boundary conditions, and finite size errors are present in all many-body calculations of extended systems. The finite size errors can be broadly classified into one-body and two-body errors. One-body errors arise due to the discrete sampling of the Brillouin zone. The two-body errors arise due to spurious correlation effects with an electron and its image in the neighboring periodic cell. In Sec. II D, we describe the corrections used in this work.

### C. Pseudopotentials

The effects of the pseudopotential approximation on the final DMC results can be significant,<sup>31</sup> and it is therefore necessary to carefully test the pseudopotentials. Previous studies have found that the effects of semi-core states are pronounced for transition metal elements.<sup>32,33</sup> Therefore, we use a Ne-core for Ni and Mn and a He-core for O. Our pseudopotentials are norm-conserving<sup>34</sup> and generated within the LDA with the OPIUM code.<sup>35</sup> Scalar relativistic effects are included in the pseudopotential construction. The nonlocal cutoff radius is constrained to be small (0.8 a.u.) to improve transferability, and the resulting potentials are quite hard. To soften the potentials to the extent possible, we use the optimization method of Rappe *et al.*<sup>36</sup> resulting in plane wave cutoff energies of 280

Ry and 269 Ry for Ni and Mn, respectively, to achieve an accuracy of 1 meV/electron.

These pseudopotentials were validated with DMC for (i) atomic ionization potentials for manganese, nickel, and oxygen and (ii) equilibrium distances and dissociation energies of MnO, NiO, and O<sub>2</sub> molecules. DMC yields ionization potentials and dissociation energies within 0.2 eV of experimental values.<sup>38</sup> The DMC equilibrium distance for MnO of 1.668(2) Å compares well with the experimental value of 1.648 Å, similar to the DMC equilibrium distance for NiO of 1.625(2) Å compared with the experimental value of 1.6271 Å. We have recently studied the magnitude of the locality and fixed-node errors in this pseudopotential family and their Jastrow sensitivities.<sup>37</sup> Additional details of our Mn, Ni, and O pseudopotentials can be found in Refs. 10 and 39.

#### D. Computational details

All DMC calculations were performed using the QMCPACK code.<sup>39</sup> Single-determinant Slater-Jastrow trial wave functions were generated with one-, two-, and three-body Jastrow factors [as represented in Eq. (1)]. All DMC calculations used the variational T-move scheme.<sup>40</sup> The single particle orbitals were generated within LDA+U<sup>5,41</sup> using a plane wave cutoff energy of 300 Ry using Quantum ESPRESSO.<sup>24</sup> Such a high cutoff energy is needed due to the hard pseudopotentials used (see Sec. II B). Unlike many studies where the value of U is chosen empirically, here we scan over U values to find those that minimize the DMC energy. In this way, we use U as a variational parameter to improve the nodal structure of the wave function since all nodal errors increase the DMC energy. When optimizing the nodes by varying the U, the magnetic primitive cell (Mn<sub>2</sub>Ni<sub>2</sub>O<sub>6</sub>) was used. A larger 2 × 2 × 1 40-atom supercell (4× the primitive magnetic cell) was used for all subsequent calculations to minimize finite size errors. DMC energies for various combinations of U values in the magnetic primitive cell are shown in Table I. From our scan, U values of 6.2 eV (Mn) and 2.9 eV (Ni) yield the lowest DMC energy and are used for all subsequent calculations. All energies are presented per formula unit.

To evaluate the equation of state (EOS) of MnNiO<sub>3</sub>, we use a time step of 0.0025 Ha<sup>-1</sup>, which converges the DMC total energy of MnNiO<sub>3</sub> to 9 mHa/formula unit. Residual time step energy differences are expected to be about an order of magnitude smaller than this. Figure 1 shows a time step

TABLE I. DMC energies per formula unit of the magnetic primitive cell for various combinations of the U parameter on Ni and Mn atoms.

U on Ni (eV)	U on Mn (eV)	DMC Energy (Ha)
5.2	2.9	-644.023 ± 0.003
5.2	3.9	-644.025 ± 0.003
5.2	4.9	-644.009 ± 0.003
6.2 <sup>a</sup>	2.9 <sup>a</sup>	-644.029 ± 0.004
6.2	3.9	-644.018 ± 0.004
6.2	4.9	-644.021 ± 0.003
7.2	2.9	-644.015 ± 0.003
7.2	3.9	-644.017 ± 0.003
7.2	4.9	-644.015 ± 0.003

<sup>a</sup>Denotes optimal values.

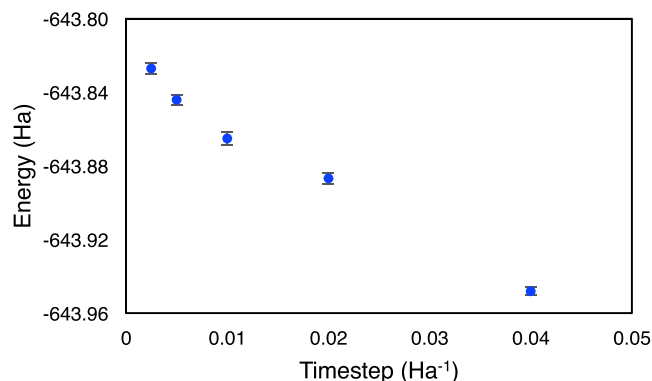


FIG. 1. Variation of the DMC total energy/formula unit with time step for the MnNiO<sub>3</sub> 2 × 2 × 1 40-atom supercell.

convergence study for the 40-atom 2 × 2 × 1 supercell of MnNiO<sub>3</sub>. We use twist-averaged boundary conditions to correct for the one-body finite-size effects,<sup>27</sup> and we use the model periodic Coulomb (MPC) interaction<sup>28–30</sup> to correct the potential energy, while the applied S(k) correction<sup>42</sup> corrects the kinetic energy. The simulation workflow was managed by Nexus.<sup>43</sup>

### III. RESULTS

#### A. Experimental

The MnNiO<sub>3</sub> crystal structure was refined using the *R*-3 space group with refined lattice parameters of  $a = 4.9076(2)$  Å and  $c = 13.5966(6)$  Å. Ni and Mn were refined in atomic positions with  $z = 0.3455(6)$  and  $z = 0.1461(6)$  and oxygen site was refined with occupancy of 1.0(2). According to EDS, there is a uniform distribution of Mn, Ni, and O elements and uniform particle sizes averaging less than 2 μm. However, the EDS averaging over a spot of sample of 753 μm diameter hints at a slightly (~5%) Mn-rich material that potentially means off-stoichiometric Ni<sub>0.95</sub>Mn<sub>1.05</sub>O<sub>3</sub>, and with Mn being smaller than Ni in terms of atomic radius, this can easily cause antisite defects. The Curie temperature ( $T_c$ ) is evident from divergent *zfc* and *fc* data and the rise in the magnetic susceptibility ( $\chi$ ) signal below  $T_c = 430$  K (Fig. 2). This value is similar to that reported in Ref. 14. The moment does not fully saturate at 4 K and 6 T (Fig. 2, inset), and the magnetization reaches a small value of ~0.3 μ<sub>B</sub>/MnNiO<sub>3</sub> formula unit, which hints at ferrimagnetic ordering. Field-dependent magnetization is linear at 750 K.

Diffuse reflection measurements were performed on a powder sample of MnNiO<sub>3</sub>, which may be slightly Mn-rich (up to ~5%) from EDS measurements. We observed an abrupt transition in reflectance in the infrared near 1600 nm (=0.78 eV), where the reflectivity at 1900 nm was 0.63 and was 0.136 at 1100 nm. According to the Kubelka-Munk theory,<sup>44</sup> the ratio of the absorption to scattering coefficient (K/S) equals 0.068 at 1900 nm and 0.373 at 1100 nm. However, the abrupt reflectance at 1600 nm is consistent with the size of the MnNiO<sub>3</sub> particles observed in a Hitachi S3400 scanning electron microscope (not shown); therefore we cannot rule out Tyndall effects to be the source of the observed reflectance.

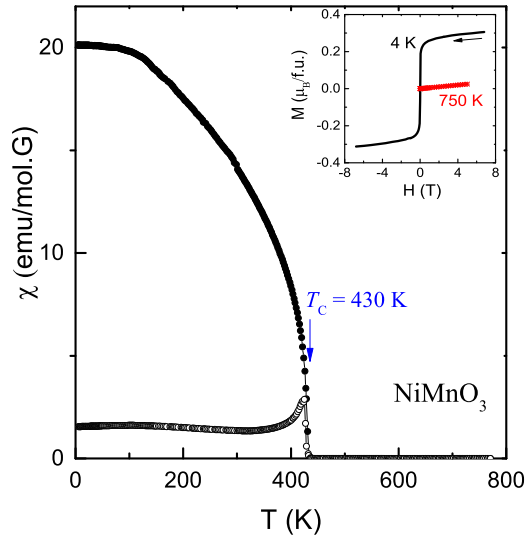


FIG. 2. Temperature-dependent magnetic susceptibility for  $\text{MnNiO}_3$ ; field-dependent magnetization is shown at 4 K and 750 K in the inset.

## B. Equation of state

To calculate the bulk modulus and equilibrium volume of solid  $\text{MnNiO}_3$ , we compute the total energy as a function of volume as shown in Fig. 3. The resulting plot is then fitted to Murnaghan's equation of state,<sup>45</sup>

$$E_T(V) = E_T(V_0) + \frac{B_0 V}{B'_0} \left[ \frac{(V_0/V)^{B'_0}}{B'_0 - 1} + 1 \right] - \frac{V_0 B_0}{B'_0 - 1}, \quad (2)$$

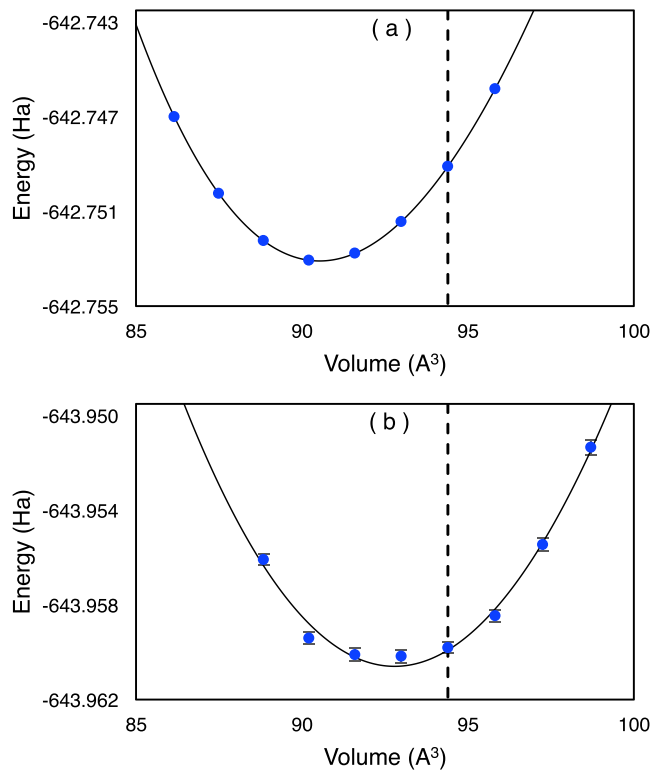


FIG. 3. Equation of states for (a) LDA+U and (b) DMC for the  $2 \times 2 \times 1$  40-atom supercell. Energies and volumes are given per formula unit. The experimental value is illustrated by the vertical dashed line.

where  $E_T(V)$  is the energy at volume  $V$ , and  $V_0$ ,  $B_0$ , and  $B'_0$  are the volume, bulk modulus, and its pressure derivative, respectively, at equilibrium. Upon fitting the computed DMC values to Eq. (2), we obtain an equilibrium volume of  $92.8 \text{ \AA}^3$  compared with the experimental value of  $94.4 \text{ \AA}^3$ . We further predict a bulk modulus of 217 GPa. Corresponding LDA+U calculated values are  $90.5 \text{ \AA}^3$  and 228 GPa.

We see an improvement in the calculated equilibrium volume using DMC (1.7% error) compared with LDA+U (4.1% error). A study on  $\text{NiO}$ <sup>11</sup> has shown a similar geometric improvement, where the error in the lattice constant went from 1.7% error (LDA+U) to 0.3% error (DMC). This can be attributed to the consistent description of the electronic correlation made in DMC, and also that geometric properties for some transition metal oxides depend strongly on the value of  $U$ .<sup>8</sup> However, errors remain, presumably due to the pseudopotential, localization, and fixed-node approximations.

## C. Band gap

The quasiparticle energy gap  $E_{qp}$  can be computed as the difference between the addition energy ( $E_A$ ) and the removal energy ( $E_R$ ) as follows:

$$\begin{aligned} E_{qp} &= E_A - E_R, \\ E_A &= E_{q^-} - E_g, \\ E_R &= E_g - E_{q^+}, \end{aligned} \quad (3)$$

where  $E_g$ ,  $E_{q^-}$ , and  $E_{q^+}$  are the DMC energies of the ground state, negatively charged state, and positively charged state of bulk  $\text{MnNiO}_3$ , respectively. This method is commonly used to calculate the quasiparticle energy gap in DMC.<sup>9,10,46–48</sup> For a more complete discussion, the reader is referred to Williamson *et al.*<sup>49</sup>

As mentioned earlier,  $\text{MnNiO}_3$  stabilizes in the ferrimagnetic ground state. Within LDA+U, we find the computed magnetic moments on Mn and Ni atoms to be  $-2.9 \mu_B$  and  $+1.7 \mu_B$ , respectively. Considering the electronic configurations of Mn and Ni atoms are  $3d^5 4s^2$  and  $3d^8 4s^2$ , respectively, the oxidation states of Mn and Ni atoms are 4+ with three  $d$ -electrons in the spin down channel while those of Ni atoms are 2+ with eight  $d$ -electrons, 5 spin up and 3 spin down. In determining the quasiparticle gaps, one can therefore create the charged states by adding or removing electrons for two separate spin channels. In Table II, we present the results for both the DMC and LDA+U calculations. We perform calculations on three supercell sizes, and the LDA+U results show a variation of about 0.2 eV between the smallest (10 atoms) and the largest supercell (40 atoms). Within DMC, we obtain

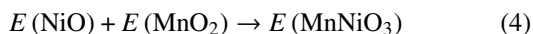
TABLE II. Quasiparticle band gaps computed with LDA+U and DMC.

Supercell size (No. of atoms)	LDA+U gap Majority (eV)	LDA+U gap Minority (eV)	DMC gap Majority (eV)	DMC gap Minority (eV)
10	1.42	2.44		
20	1.30	2.31		
40	1.24	2.42	2.01	3.83

quasiparticle gaps of 2.0(5) eV and 3.8(6) eV for majority and minority spin channels, respectively.

#### D. Oxygen vacancy, antisite formation, and Mn-rich conditions

It has proven to be challenging to synthesize pure MnNiO<sub>3</sub>. Calculations were performed to rationalize which impurities in MnNiO<sub>3</sub> are more likely. Using previously calculated energies for MnO<sub>2</sub><sup>50</sup> and NiO,<sup>51</sup> the reaction



gives a formation energy of -0.997 eV (LDA+U) and -1.857(1) eV (DMC) per formula unit. The formation of an antisite pair, where one Mn swaps location with one Ni, costs +2.021 eV (LDA+U) and +2.8(1) eV (DMC). The formation of an oxygen vacancy by the reaction



is found to be +3.751 eV (LDA+U). This corresponds to approximately a 4% concentration of oxygen vacancies (not extrapolated to the low-density limit). In oxygen-rich conditions, we have

$$\mu_{\text{O}(\text{rich})} = \frac{E(\text{O}_2)}{2}. \quad (6)$$

In oxygen-poor conditions, we have

$$\mu_{\text{O}(\text{poor})} = E(\text{MnNiO}_3) - E(\text{NiO}) - E(\text{MnO}). \quad (7)$$

We find  $\Delta(\mu_{\text{O}(\text{rich})} - \mu_{\text{O}(\text{poor})})$  to be +2.624 eV (LDA+U). We also compare the gaps between bulk MnNiO<sub>3</sub>, MnNiO<sub>3</sub> containing an antisite pair, and the Mn-rich conditions Mn<sub>1.06</sub>Ni<sub>0.94</sub>O<sub>3</sub> that more closely reflect the experimental stoichiometry. We find that while there is a well-defined gap for the bulk MnNiO<sub>3</sub>, MnNiO<sub>3</sub> with an antisite pair and Mn antisite Mn<sub>1.06</sub>Ni<sub>0.94</sub>O<sub>3</sub> are both metallic in LDA+U.

#### IV. CONCLUSION

In this work, we present new experimental data and *ab initio* results for MnNiO<sub>3</sub>. High-level diffusion quantum Monte Carlo calculations resolve the functional-dependent discrepancies in previous reports using approximations of density functional theory. DMC reproduces the experimental results available accurately and provides insight into the experimentally observed imperfect stoichiometry.

We have theoretically and experimentally revisited a relatively unexplored material—MnNiO<sub>3</sub>—and considered its properties as a potential photocatalyst. We performed highly accurate diffusion quantum Monte Carlo calculations of the equation of state and the quasiparticle band gaps for minority and majority spins of MnNiO<sub>3</sub>. We synthesized MnNiO<sub>3</sub> as evidenced by the lattice structure. Experimentally, the ferromagnetism found in MnNiO<sub>3</sub> ( $T_c = 430$  K) is consistent with previous reports. A defective material seems to form with potential oxygen vacancies and Ni and Mn off-stoichiometries, which cause antisite defects. We found that the theory and experiment agree very well for the structural properties and noted an improvement of 2.4% in the calculated equilibrium volume using DMC compared with LDA+U due to the accurate treatment of the electron correlation in DMC. Despite this

improvement, the DMC-calculated volume is still not reaching the experimental value. Common sources of suspected errors are the fixed-node approximation, the pseudopotentials, and locality errors in the pseudopotential evaluations. Locality errors can be reduced in the future since our Jastrow factors are within an atomic picture. Adding electron-ion-ion terms and/or electron-electron-ion-ion terms to the wave function could reduce locality errors. However, Jastrow terms of this form are not yet available in QMCPACK.

The calculated excitation band gap obtained with DMC without adjustable parameters was found to be 2.0(5) eV, somewhere in between the calculated values obtained with empirically adjusted functionals [LDA+U (1.75 eV) and HSE (2.98 eV)].<sup>1</sup> Calculated DMC band gaps can be used to determine which functional is more appropriate for this class of materials. The experimental determination of the optical properties was hindered by the difficulty to control the Mn/Ni ratio and to simultaneously produce large enough (mm) insulating crystals. We find theoretically that the formation energy of an antisite pair, an exchange of two neighboring atoms of Ni and Mn, costs approximately 1 eV less than the formation of an oxygen vacancy. We find that these antisite pairs, as well as any departure from the perfect stoichiometry turn the material metallic-like.

#### ACKNOWLEDGMENTS

The authors are grateful to Michael McGuire for helpful discussions. This work was supported by the Materials Science and Engineering Division of the U.S. Department of Energy Office of Science (BES). This research used resources of the Oak Ridge Leadership Computing Facility at the Oak Ridge National Lab, which is supported by the Office of Science of the U.S. Department of Energy under Contract No. DE-AC05-00OR22725.

This manuscript has been authored by UT-Battelle, LLC under Contract No. DE-AC05-00OR22725 with the U.S. Department of Energy. The United States Government retains and the publisher, by accepting the article for publication, acknowledges that the United States Government retains a non-exclusive, paid-up, irrevocable, worldwide license to publish or reproduce the published form of this manuscript, or allow others to do so, for United States Government purposes. The Department of Energy will provide public access to these results of federally sponsored research in accordance with the DOE Public Access Plan (<http://energy.gov/downloads/doe-public-access-plan>).

<sup>1</sup>J. Yu, Q. Yan, W. Chen, A. Jain, J. B. Neaton, and K. A. Persson, *Chem. Commun.* **51**, 2867 (2015).

<sup>2</sup>W. Kohn and L. J. Sham, *Phys. Rev.* **140**, A1133 (1965).

<sup>3</sup>J. P. Perdew and W. Yue, *Phys. Rev. B* **33**, 8800 (1986).

<sup>4</sup>L. K. Wagner and D. M. Ceperley, *Rep. Prog. Phys.* **79**, 094501 (2016).

<sup>5</sup>V. I. Anisimov, J. Zaanen, and O. K. Andersen, *Phys. Rev. B* **44**, 943 (1991).

<sup>6</sup>V. I. Anisimov, I. V. Solovyev, M. A. Korotin, M. T. Czyzyk, and G. A. Sawatzky, *Phys. Rev. B* **48**, 16929 (1993).

<sup>7</sup>A. I. Liechtenstein, V. I. Anisimov, and J. Zaanen, *Phys. Rev. B* **52**, R5467 (1995).

<sup>8</sup>J. A. Santana, J. Kim, P. R. C. Kent, and F. A. Reboredo, *J. Chem. Phys.* **141**, 164706 (2014).

<sup>9</sup>E. Ertekin, L. K. Wagner, and J. C. Grossman, *Phys. Rev. B* **87**, 155210 (2013).

- <sup>10</sup>J. A. Santana, J. T. Krogel, J. Kim, P. R. C. Kent, and F. A. Reboredo, *J. Chem. Phys.* **142**, 164705 (2015).
- <sup>11</sup>C. Mitra, J. T. Krogel, J. A. Santana, and F. A. Reboredo, *J. Chem. Phys.* **143**, 164710 (2015).
- <sup>12</sup>J. Yu, L. K. Wagner, and E. Ertekin, *Phys. Rev. B* **95**, 075209 (2017).
- <sup>13</sup>J. A. Santana, J. T. Krogel, P. R. C. Kent, and F. A. Reboredo, *J. Chem. Phys.* **147**, 034701 (2017).
- <sup>14</sup>A. Feltz and J. Töpfer, *J. Alloys Compd.* **196**, 75 (1993).
- <sup>15</sup>W. H. Cloud, *Phys. Rev.* **111**, 1046 (1958).
- <sup>16</sup>H. S. Jarrett and R. K. Waring, *Phys. Rev.* **111**, 1223 (1958).
- <sup>17</sup>E. F. Bertaut and F. Forrat, *J. Appl. Phys.* **29**, 247 (1958).
- <sup>18</sup>R. Grimm and R. Storer, *J. Comput. Phys.* **7**, 134 (1971).
- <sup>19</sup>J. B. Anderson, *J. Chem. Phys.* **63**, 1499 (1975).
- <sup>20</sup>W. M. C. Foulkes, L. Mitas, R. J. Needs, and G. Rajagopal, *Rev. Mod. Phys.* **73**, 33 (2001).
- <sup>21</sup>R. J. Needs, M. D. Towler, N. D. Drummond, and P. L. Ríos, *J. Phys.: Condens. Matter* **22**, 023201 (2010).
- <sup>22</sup>W. L. McMillan, *Phys. Rev.* **138**, A442 (1965).
- <sup>23</sup>R. Jastrow, *Phys. Rev.* **98**, 1479 (1955).
- <sup>24</sup>P. Giannozzi, S. Baroni, N. Bonini, M. Calandra, R. Car, C. Cavazzoni, D. Ceresoli, G. L. Chiarotti, M. Cococcioni, I. Dabo, A. Dal Corso, S. de Gironcoli, S. Fabris, G. Fratesi, R. Gebauer, U. Gerstmann, C. Gougoussis, A. Kokalj, M. Lazzeri, L. Martin-Samos, N. Marzari, F. Mauri, R. Mazzarello, S. Paolini, A. Pasquarello, L. Paulatto, C. Sbraccia, S. Scandolo, G. Sclauzero, A. P. Seitsonen, A. Smogunov, P. Umari, and R. M. Wentzcovitch, *J. Phys.: Condens. Matter* **21**, 395502 (2009).
- <sup>25</sup>D. M. Ceperley and B. J. Alder, *Phys. Rev. Lett.* **45**, 566 (1980).
- <sup>26</sup>M. H. Kalos, D. Levesque, and L. Verlet, *Phys. Rev. A* **9**, 2178 (1974).
- <sup>27</sup>C. Lin, F. H. Zong, and D. M. Ceperley, *Phys. Rev. E* **64**, 016702 (2001).
- <sup>28</sup>N. D. Drummond, R. J. Needs, A. Sorouri, and W. M. C. Foulkes, *Phys. Rev. B* **78**, 125106 (2008).
- <sup>29</sup>L. M. Fraser, W. M. C. Foulkes, G. Rajagopal, R. J. Needs, S. D. Kenny, and A. J. Williamson, *Phys. Rev. B* **53**, 1814 (1996).
- <sup>30</sup>A. J. Williamson, G. Rajagopal, R. J. Needs, L. M. Fraser, W. M. C. Foulkes, Y. Wang, and M.-Y. Chou, *Phys. Rev. B* **55**, R4851 (1997).
- <sup>31</sup>L. Shulenburger and T. R. Mattsson, *Phys. Rev. B* **88**, 245117 (2013).
- <sup>32</sup>K. Foyevtsova, J. T. Krogel, J. Kim, P. R. C. Kent, E. Dagotto, and F. A. Reboredo, *Phys. Rev. X* **4**, 031003 (2014).
- <sup>33</sup>L. Mitas, E. L. Shirley, and D. M. Ceperley, *J. Chem. Phys.* **95**, 3467 (1991).
- <sup>34</sup>D. R. Hamann, M. Schlüter, and C. Chiang, *Phys. Rev. Lett.* **43**, 1494 (1979).
- <sup>35</sup>See <http://opium.sourceforge.net/sci.html> for Opium: Pseudopotential generation project.
- <sup>36</sup>A. M. Rappe, K. M. Rabe, E. Kaxiras, and J. D. Joannopoulos, *Phys. Rev. B* **41**, 1227 (1990).
- <sup>37</sup>A. L. Dzubak, J. T. Krogel, and F. A. Reboredo, *J. Chem. Phys.* **147**, 024102 (2017).
- <sup>38</sup>J. T. Krogel, J. A. Santana, and F. A. Reboredo, *Phys. Rev. B* **93**, 075143 (2016).
- <sup>39</sup>J. Kim, K. P. Esler, J. McMinis, M. A. Morales, B. K. Clark, L. Shulenburger, and D. M. Ceperley, *J. Phys.: Conf. Ser.* **402**, 012008 (2012).
- <sup>40</sup>M. Casula, *Phys. Rev. B* **74**, 161102 (2006).
- <sup>41</sup>M. Cococcioni and S. de Gironcoli, *Phys. Rev. B* **71**, 035105 (2005).
- <sup>42</sup>S. Chiesa, D. Ceperley, R. Martin, and M. Holzmann, *Phys. Rev. Lett.* **97**, 076404 (2006).
- <sup>43</sup>J. T. Krogel, *Comput. Phys. Commun.* **198**, 154 (2016).
- <sup>44</sup>P. Kubelka and F. Munk, *Z. Tech. Phys.* **12**, 593 (1931).
- <sup>45</sup>F. D. Murnaghan, *Proc. Natl. Acad. Sci. U. S. A.* **30**, 244 (1944).
- <sup>46</sup>J. Kolorenc and L. Mitas, *Phys. Rev. Lett.* **101**, 185502 (2008).
- <sup>47</sup>M. Abbasnejad, E. Shojaei, M. R. Mohammadzadeh, M. Alaei, and R. Maezono, *Appl. Phys. Lett.* **100**, 261902 (2012).
- <sup>48</sup>L. K. Wagner and P. Abbamonte, *Phys. Rev. B* **90**, 125129 (2014).
- <sup>49</sup>A. J. Williamson, R. Q. Hood, R. J. Needs, and G. Rajagopal, *Phys. Rev. B* **57**, 12140 (1998).
- <sup>50</sup>V. Sharma, J. T. Krogel, P. R. C. Kent, and F. A. Reboredo, "Diffusion Monte Carlo: A pathway towards an accurate theoretical description of Mn oxides" (unpublished).
- <sup>51</sup>H. Shin, Y. Luo, P. Ganesh, J. Balachandran, J. T. Krogel, P. R. C. Kent, A. Benali, and O. Heinonen, "Electronic properties of doped and defective NiO—A quantum Monte Carlo study" (unpublished).